The aromatic cluster in KCHIP1b affects Kv4 inactivation gating

D. Van Hoorick, A. Raes and D. J. Snyders

Laboratory for Molecular Biophysics, Physiology and Pharmacology, Department of Biomedical Sciences, University of Antwerp, Universiteitsplein 1, 2610 Antwerp, Belgium

The KChIP1b splice variant has been shown to induce slow recovery from inactivation for Kv4.2 whereas KChIP1a enhanced the recovery. Both splice variants differ only by the insertion of the exon1b, rich in aromatic residues (5/11). We analysed in detail the modifications of Kv4.2 gating induced by the KChIP1b splice variant and the role for the aromatic cluster in KChIP1b in inducing these changes. By substituting alanine for the aromatic residues individually or in combination, we could convert the KChIP1b recovery behaviour into that of KChIP1a. The replacement of one or two aromatic residues resulted in a partial restitution of the KChIP1a recovery behaviour. When three aromatic residues were replaced in the exon1b, the recovery from inactivation was fast with time constants that were similar to those obtained with KChIP1a. Moreover, similar findings were observed for closed state inactivation and for the voltage dependence of inactivation. Thus, reduction of the side chain bulkiness in exon1b resulted in the conversion of the KChIP1b phenotype into the KChIP1a phenotype. These results indicate that the aromatic cluster in exon1b modulates the transitions towards and from the closed inactivated states and the steady state distribution over the respective states.

(Resubmitted 26 June 2007; accepted 17 July 2007; first published online 26 July 2007)
Corresponding author D. J. Snyders: Laboratory for Molecular Biophysics, Physiology and Pharmacology, Department of Biomedical Sciences, University of Antwerp, Universiteitsplein 1, 2610 Antwerp, Belgium. Email: dirk.snyders@ua.ac.be

The A-type K^+ channels are characterized by a rapid activation starting from subthreshold voltages followed by rapid and complete inactivation usually combined with quick recovery from inactivation. These features are essential for their function in neuronal behaviour in dampening the excitability, preventing back propagation and setting the threshold for spike initiation (Yuste, 1997; Hoffman *et al.* 1997; Schoppa & Westbrook, 1999). Several A-type channels exist and the channels associate *in vivo* with auxiliary subunits to form a macromolecular complex. The KChIP family was identified as interaction partner of the Kv4 subfamily of voltage gated K^+ channel α-subunits (An *et al.* 2000). Most of the KChIP subunits have comparable effects on the Kv4 channels: up-regulation of the current density, slowing of inactivation and acceleration of recovery from inactivation (An *et al.* 2000; Decher *et al.* 2001; Bahring *et al.* 2001*b*). Another proposed constituent of the native A-type channel complexes is the DPPX protein, a member of a large family of dipeptidyl aminopeptidases (Nadal *et al.* 2003; Radicke *et al.* 2005; Jerng *et al.* 2005). This protease-like protein interacts with Kv4 channels and most likely interacts *in vivo* with Kv4 to form native A-type channels.

Several researchers have performed a detailed characterization of the Kv4 inactivation and have tried to model the different gating transitions because a thorough understanding of the inactivation process is essential to comprehend the functioning of A-type channels (Bahring *et al.* 2001*a*; Beck *et al.* 2002; Patel *et al.* 2004; Jerng *et al.* 2004). There is a consensus on the fact that different inactivation pathways exist in Kv4, originating from a closed state and originating from the open state. However, there is still controversy on the proper gating model and the interpretation of the different time constants obtained experimentally. The Kv4 channel gating is even more complicated by the presence of auxiliary subunits, such as KChIPs.

We identified a splice variant of KChIP1, KChIP1b, that showed remarkable effects on the recovery from inactivation (Van Hoorick *et al.* 2003). Whereas most KChIP isoforms enhance the recovery from inactivation, this splice variant slows the recovery from inactivation by the induction of a second slow component. Slowing of recovery from inactivation has also been described for KChIP2g although here the recovery from inactivation could be described by a single exponential function

This paper has online supplemental material.

 DOI: 10.1113/jphysiol.2007.139550

(Decher *et al.* 2004). For the KChIP4a isoform the presence of a KIS domain in the amino terminus of the protein results in Kv4 recovery from inactivation that is unaltered upon cotransfection (Holmqvist *et al.* 2002). Most of the diversity between the different KChIPs resides in their amino terminus whereas the C-terminal half is more conserved. Although it has been reported for a KChIP2 splice variant that the conserved half of the protein was sufficient to reproduce all aspects of modulation, it is remarkable that many splice variants exist often only differing in their amino terminus (Patel *et al.* 2002).

Here, we analyse in more detail the gating effects of KChIP1b and try to correlate these effects to the structural differences between KChIP1a and KChIP1b. We therefore first compared the effects of KChIP1a and KChIP1b on the Kv4.2 gating. These results were incorporated in a computer model, adapted from a previously published model (Beck *et al.* 2002). Next, an alanine mutation scan was conducted across the inserted exon1b of the KChIP1b splice variant to determine the contribution of the aromatic cluster in exon1b to the KChIP1b modulation of Kv4 gating. Individual aromatic residues were replaced by substituting alanine, followed by combinations of the different mutations. Based upon these mutations we can conclude that the aromatic residues contribute significantly to the functional effects of the KChIP1b splice variant.

Methods

Molecular biology

Mouse KChIP1a and KChIP1b cDNAs were obtained from a mouse brain cDNA library isolated in our laboratory as previously described (Van Hoorick *et al.* 2003). The following primers with flanking restriction sites (lower case) were used for amplification: 5′-cttaagctt-AAGACGCACACAAGTCTTC-3′ and 5′-ataggatcca-TTACATGACATTTTGGAACAGC-3′. These primers were based on the EST sequences with accession numbers BG293918 and BE652426. PCR products were cut with *Hin*dIII and *Bam*HI before directional ligation into the pEGFP-vector (Clontech, Mountain View, CA, USA). Alanine substitutions were performed with the site directed mutagenesis kit (Stratagene, La Jolla, CA, USA). Flanking mutations were inserted during a single PCR run. Double stranded sequencing was done to confirm the intended mutation and the absence of unwanted mutations.

Transfection

All experiments were conducted in Ltk$^-$ cells. Culturing conditions of the Ltk$^-$ cells and the generation of the stable cell line have been previously described (Yeola & Snyders, 1997). Transfections were performed on cultures at 70% confluency with Lipofectamine (Invitrogen, Carlsbad, CA, USA) according to the manufacturer's instructions. For electrophysiological analysis, a cell line with stable Kv4.2 expression was transfected with 3 μg KChIP DNA where indicated. A GFP marker (0.5 μg) was cotransfected in order to select transfected cells for electrophysiology by their GFP fluorescence.

Whole cell current recording, pulse protocols and data analysis

Current recordings were made in the whole cell configuration of the patch-clamp technique (Hamill *et al.* 1981). Details of the pulse protocols are specified in the figure legends. To obtain the voltage dependence of isochronal inactivation, the peak current amplitude at +50 mV was plotted as a function of the prepulse voltage and different conditioning step lengths were used. The voltage dependencies of activation or inactivation were fitted with a Boltzmann equation according to $y = 1/(1 + \exp(-(V - V_{1/2})/k))$, where $V_{1/2}$ represents the voltage at which 50% of the channels are open or inactivated and k is the slope factor. Recovery and inactivation kinetics were fitted with a single or double exponential function using a nonlinear least-squares (Gauss–Newton) algorithm. Goodness of fit and required number of exponential components was judged by comparing residuals and F statistics. Results are expressed as means ± S.E.M. Student's paired t test was used to compare the differences in mean values; $P < 0.05$ was considered significant. In the case of a difference in the variances of both populations, a Mann–Whitney rank sum test was used. Simulations were performed based on the model of Beck *et al.* (2002) with adjustments of rate constants as explained in Results. The Markov model was solved using the Q-matrix approach in the Matlab package (version 7, The Mathworks, Natick, MA, USA).

The terms 'open state inactivated state' and 'closed inactivated state' are used as shorthand for inactivated states reached from the open and closed state, respectively.

Results

We previously reported the identification of a novel splice variant of KChIP1, termed KChIP1b, and described its effects on Kv4.2 channels with the most prominent modulation being a distinctive slowing of the recovery from inactivation (Van Hoorick *et al.* 2003). To investigate the role of the aromatic cluster that characterizes the KChIP1b splice variant, we analysed the effects of KChIP1b and its mutants after cotransfection on a Kv4.2 expressing stable cell line.

Inactivation of macroscopic currents

Upon long depolarizations (2–5 s), Kv4 channels inactivate completely by a process that has been described by a double or triple exponential function by different researchers (Bahring *et al.* 2001*a*; Beck *et al.* 2002; Patel *et al.* 2004; Wang *et al.* 2005). Such differences in analysis may originate from variations in the expression system used or from the observed current amplitude. A low current density may preclude the observation of a small third component. The stable cell line used in this study expressed a modest Kv4.2 current (26.4 ± 1.7 pA pF^{-1} at +50 mV) allowing adequate voltage control of the up regulated Kv4.2 currents upon KChIP coexpression. Cells were held at −90 mV and the current was activated by 5 s pulses to potentials between −20 and +50 mV in 10 mV steps. Representative recordings of the different transfections are shown in the upper panels of Fig. 1. As mentioned earlier, inactivation of macroscopic currents is sometimes described by a triple exponential function. However, under our experimental conditions attempts to fit the current decay to a triple exponential function resulted in negative initial amplitudes for the third component. Macroscopic inactivation was therefore analysed by fitting a double exponential function to the inactivating part of the current traces. The resulting time constants and their fractional amplitudes are shown in Fig. 2*A* and *B*. For Kv4.2 the fast component displayed a clear voltage dependence and represented approximately 90% of the decay (Fig. 2). The slow component showed minimal voltage dependence over the entire voltage range tested. Cotransfection of KChIP1a resulted in an enhancement of the slow component and a slowing of the fast component of inactivation. The contribution of the slow component increased from 10 to 40% between −10 and +60 mV. Transfection of KChIP1b on the other hand resulted in a slowing of the fast component and a more limited enhancement of the slow component that represented 30% of the amplitude between +10 and +60 mV with lesser voltage dependence. Overall this resulted in both cases in a slowing of inactivation upon coexpression of Kv4.2 with KChIP1a or KChP1b.

Deactivation

After a short 5 ms pulse to +50 mV channels were allowed to deactivate at different potentials (−110 mV to −50 mV). The deactivating tails were analysed by fitting them with a single exponential function and the resulting time constants are shown in Fig. 2*C*. Limited voltage dependence of deactivation kinetics was noted at potentials more negative than −80 mV. In the presence of KChIPs the rate of deactivation was equally enhanced for both splice variants.

Recovery from inactivation

The recovery from inactivation was analysed using a twin pulse protocol as shown in the upper part of Fig. 3*A*. Channels were inactivated during a test pulse to +50 mV and allowed to recover from inactivation for different time intervals. The extent of recovery was assessed by comparing the amplitude of the current in the second test pulse to the amplitude obtained in the reference pulse. Representative traces are shown in Fig. 3*A*. At −90 mV the recovery from inactivation could be described adequately by a single exponential function for Kv4.2 alone or in the presence of KChIP1a (Table 1). However, upon coexpression of KChIP1b a double exponential function was required to describe the recovery from inactivation accurately as noted previously (Table 1) (Van Hoorick *et al.* 2003). Even after longer depolarizing pulses (5 s) the Kv4.2 recovery from inactivation in the presence of

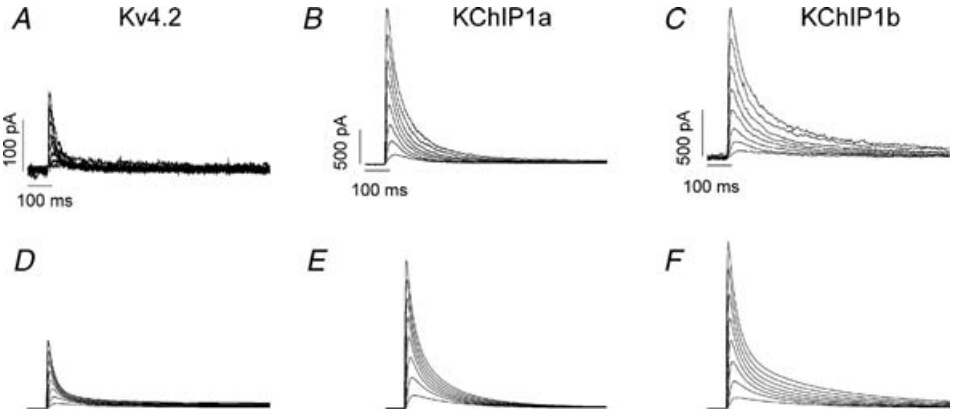

Figure 1. Inactivation of Kv4.2 in the absence or presence of KChIP1a/b subunits
A–C, representative current traces for Kv4.2, Kv4.2 + KChIP1a and Kv4.2 + KChIP1b, respectively. Inactivation was elicited during 1 s depolarizing pulses to potentials between +50 mV and −20 mV in 10 mV decrements. *D–F*, traces from the model simulation corresponding with the traces above.

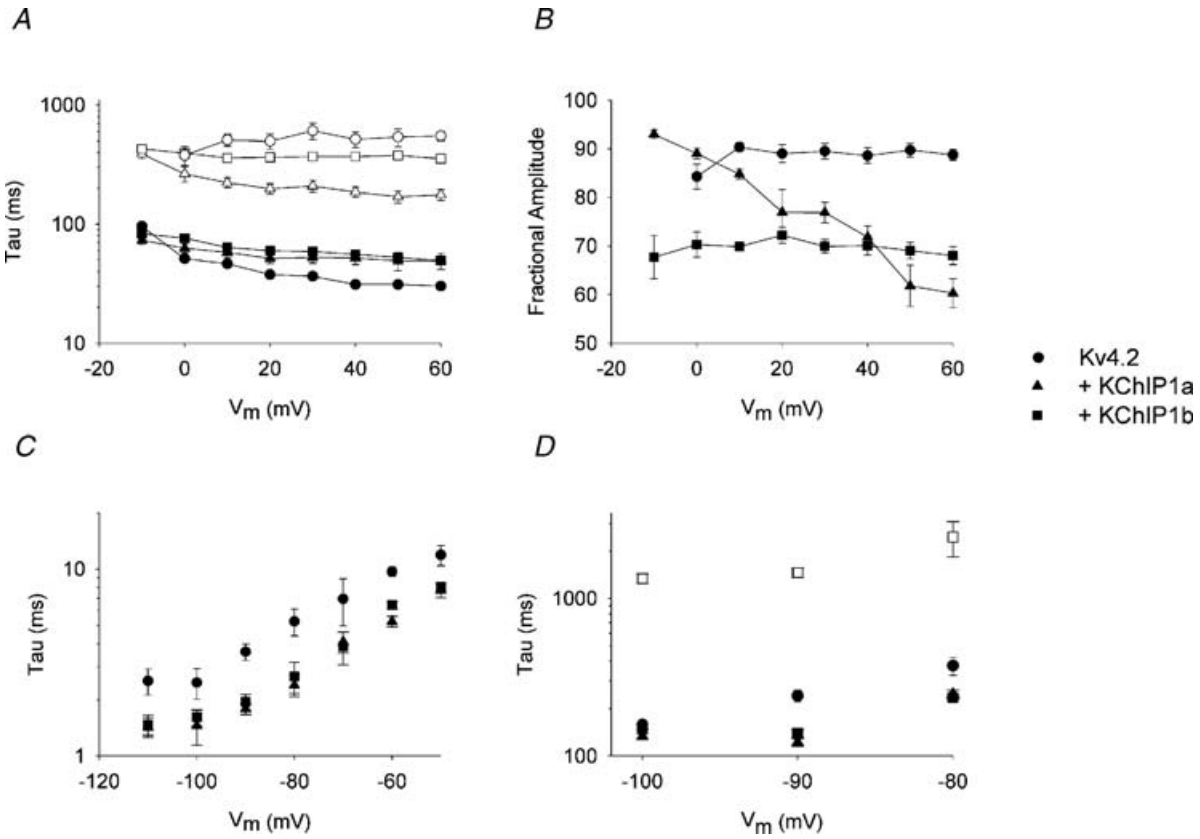

Figure 2. Kinetics of Kv4.2 in the absence or presence of KChIP1a/b
A, time constants of inactivation determined from traces as shown in Fig. 1. Under all conditions a double exponential function was used. *B*, relative contribution of the fast time constant. *C*, time constants of deactivation. *D*, voltage dependence of recovery from inactivation. When needed open symbols were used to represent the slow component of the exponential fits.

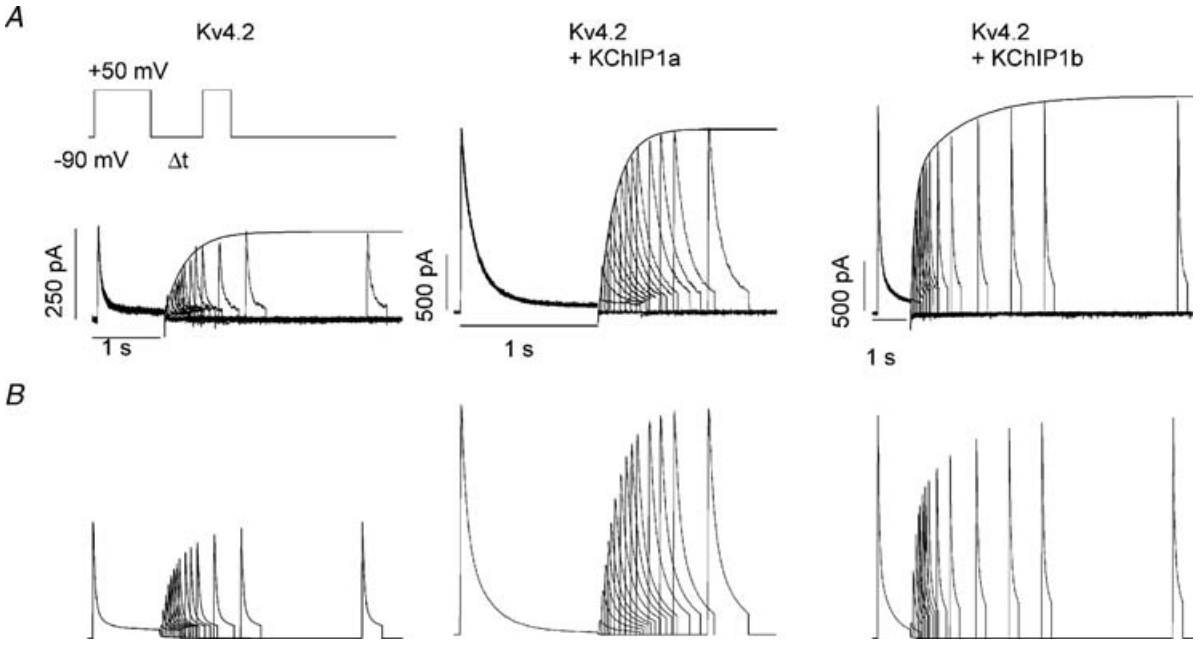

Figure 3. Recovery from inactivation
A, typical current traces of recovery from inactivation for the different conditions. The applied protocol is shown as an insert in *A*. Notice the difference in time scale between KChIP1a and KChIP1b. *B*, computer simulations based on the model in Fig. 5 of the respective conditions.

Table 1. Time constants of recovery from inactivation

													Recovery			
Residu no.	21	22	23	24	25	26	27	28	29	30	31	τ_1	*n*	τ_1	τ_2	$A_2/(A_1+A_2)$	*n*
WT-exon1b	D	I	A	W	W	Y	Y	Q	Y	Q	R	—	—	140 ± 8	1504 ± 106	45 ± 3	9
W24A				A								—	—	128 ± 18	968 ± 82*	33 ± 4	7
W25A					A							—	—	138 ± 13	964 ± 90*	34 ± 2	7
Y26A						A						—	—	145 ± 16	1091 ± 87*	43 ± 6	6
Y27A							A					—	—	129 ± 5	1284 ± 151	35 ± 4	6
Y29A									A			—	—	156 ± 16	1276 ± 165	35 ± 10	5
Mutant 1				A	A							190 ± 17	6	122 ± 12	604 ± 105*	28 ± 3	6
Mutant 2						A	A					181 ± 27	6	87 ± 13*	609 ± 151*	43 ± 6	6
Mutant 3							A		A			181 ± 19	7	83 ± 12*	523 ± 51*	35 ± 2	7
Mutant 4				A	A	A						97 ± 6	18	—	—	—	—
Mutant 5					A	A	A					122 ± 14	8	—	—	—	—
Mutant 6						A	A		A			144 ± 15	6	—	—	—	—
Mutant 7				A			A		A			159 ± 18	4	—	—	—	—
Mutant 8				A	A	A	A		A			100 ± 15	7	—	—	—	—
KChIP1a												119 ± 8	11	—	—	—	—
Kv4.2												242 ± 20	15	—	—	—	—

*Significant different from KChIP1b ($P < 0.05$).

KChIP1b remained a double exponential process (online supplemental material, Supplemental Fig. 1). The time constants (τ_1: 170 ± 30 ms, τ_2: 1490 ± 110 ms, $n = 5$) corresponded well with the time constants obtained after a 1 s depolarizing pulse although the contribution of the slow component increased upon longer depolarization ($A_2/A_1 + A_2$: 67 ± 3). Similar results were observed at −80 and −100 mV: KChIP1b coexpression always required a double exponential function to describe recovery from inactivation (Fig. 2*D*). However, for Kv4.2 alone or in the presence of KChIP1a a single exponential function sufficed. The fast component of the recovery in the presence of KChIP1b corresponded to the time constant of recovery obtained in the presence of KChIP1a. These results suggest that, compared to the recovery of Kv4.2, the recovery with KChIP1b is enhanced in a similar fashion as in the presence of KChIP1a but with the occurrence of a slow component.

Prepulse inactivation

The prepulse inactivation was analysed with a four pulse protocol as previously described (Beck & Covarrubias, 2001; Wang *et al.* 2005). The maximal current amplitude was determined in a reference pulse to +50 mV. After a 10 s recovery period at −90 mV, prepulse inactivation was induced by subtreshold conditioning steps to −50 mV of different durations (up to 14 s) followed by a test pulse to +50 mV to assess the amount of inactivation induced (see Fig. 4*A*). The amplitude obtained in the second test pulse was normalized to the amplitude of the preceding reference pulse. Upon expression of KChIP1a the 'closed state' inactivation process showed a single exponential decay with a time constant, τ, of 968 ± 192 ms ($n = 9$). The coexpression of KChIP1b and Kv4.2 on the other hand resulted in a double exponential decay with the following time constants: $\tau_1 = 411 \pm 36$ ms, $\tau_2 = 3028 \pm 410$ ms ($n = 8$). Representative current traces are shown in Fig. 4*B* and *C*. This indicated that the presence of the aromatic cluster also influenced the induction of closed state inactivation. This was previously not observed for KChIP1b due to the use of a different protocol with limited lengths of the conditioning step to −50 mV.

Computer simulations

Based upon our results and published data, a computer model was adapted to describe and interpret our experimental data (Fig. 5). Comparison of several published computer models revealed that the model described by Beck *et al.* (2002) could most readily be adapted to reproduce our experimental data. We included an additional inactivated state termed I_7 connected to the final closed inactivated state. For Kv4.2 channels without KChIPs we adapted the original model as follows: the voltage dependence of activation was shifted to reproduce our experimental data and the rate constants of inactivation were slightly modified to approximate more closely our Kv4.2 kinetics. State I_7, included for the approximation of the KChIP data, was not occupied. To reproduce the modulation of Kv4.2 inactivation by KChIPs, changes in K_{OI}, K_{IO}, K_{56} and K_{CI} were necessary. For the reproduction of the KChIP1a or KChIP1b modulation of Kv4.2 recovery from inactivation, the additional state was included in the gating scheme. In the presence of KChIP1a, the backward rate from I_7 was fast

resulting in an overall single exponential recovery from inactivation. In the presence of KChIP1b the backward rate was much slower resulting in a significant number of channels residing in I_7 and causing the double exponential recovery from inactivation. Furthermore the enhancement of the transitions to I_4 (K_{CI}) was smaller compared to the enhancement in the presence of KChIP1a.

Current traces obtained by the computational simulations are shown in Figs 1*D–F* and 3*B*. From these simulations it can be seen that the model accurately described our experimental data.

Mutational analysis of exon1b

Although the KChIP1a and the KChIP1b splice variants differ only by the insertion of an extra exon of 11 amino acids, they do have characteristic and different effects on the gating of Kv4.2 channels as shown above. Aromatic residues in the exon1b of KChIP1b have large side chains that could interact with other parts of the KChIP1 protein or with the Kv4 protein. Because of this striking feature the aromatic residues were replaced by substituting alanines individually and in various combinations to investigate their role on Kv4 inactivation.

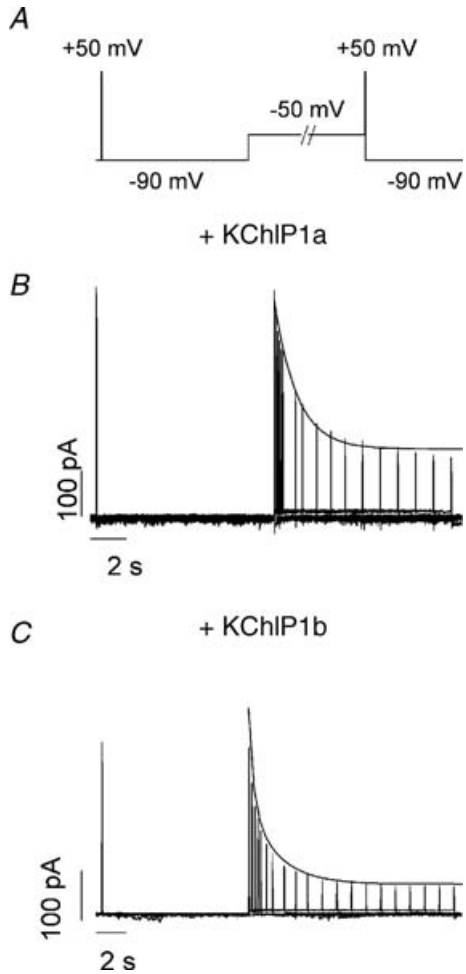

Figure 4. Prepulse inactivation of Kv4.2
B, the prepulse inactivation of Kv4.2 obtained in the presence of KChIP1a subunits upon application of the protocol depicted in *A*. *C*, transfection of the wild-type KChIP1b protein resulted in a double exponential inactivation compared to a single exponential process in the presence of KChIP1a. The continuous lines represent exponential fits to the data.

Recovery from inactivation

Substitution of alanine for individual aromatic residues in the exon1b was already sufficient to alter the recovery kinetics. Replacement of tryptophan 24 or 25 (W24A and W25A) enhanced the recovery from inactivation mainly by speeding up the slow component (Table 1) and reducing the contribution of the slow component. The substitution of alanine for tyrosines 26, 27 or 29 (Y26A, Y27A and Y29A) resulted in a more modest enhancement of the recovery from inactivation. The slow time constant was only slightly enhanced while its contribution was lowered, with exception of the Y26A mutation where the contribution of the slow time constant did not alter. All single substitutions for aromatic residues thus resulted in a recovery behaviour that was best described by a double exponential function. Therefore, the removal of a single aromatic side chain moderately affected the KChIP1b recovery phenotype but did not eliminate the second component in the recovery from inactivation.

Subsequently, combinations of the different substitutions were made to test for larger effects on the recovery from inactivation. Mutant 1 represents the replacement of the tryptophans at positions 24 and 25 and resulted in a recovery behaviour that was best described by a double exponential function for some recordings while for others of the same mutant a single exponential function was preferred based on *F*-statistics. Typical recordings of the observed recovery behaviour are shown in Fig. 6. The combination of two other aromatic residues (mutant 2 and mutant 3) also resulted in an intermediate recovery behaviour (Table 1). The combined replacement of two tyrosine residues also enhanced the recovery by significantly reducing the slow time constant to values around 600 ms, compared to the value of approximately 1500 ms in the presence of wild-type KChIP1b (for detailed statistics see Table 1).

A complete restitution of the KChIP1a recovery behaviour was observed with mutants in which at least three aromatic residues were replaced (mutants 4, 5, 6 and 7, see Table 1). When expressed with Kv4.2 these mutants showed a recovery from inactivation identical to the recovery from inactivation observed with KChIP1a: instead of the double exponential recovery a single exponential function could adequately describe

the recovery from inactivation. The replacement of all aromatic residues (mutant 8) also resulted in a monoexponential behaviour of recovery from inactivation, comparable to that seen in the presence of KChIP1a. Taken together, these data indicate that the removal of at least three aromatic residues in the exon1b could convert the recovery from inactivation from the KChIP1b phenotype into that of KChIP1a, independent of the exact location of the aromatic residues targeted.

Prepulse inactivation

When three aromatic residues were replaced (KChIP1b-mutant 4) the time course of prepulse inactivation was comparable to that seen upon coexpression with KChIP1a subunits, i.e. a single exponential process with time constants $\tau_1 = 1377 \pm 127$ ms ($n = 10$, $P = 0.09$ compared to KChIP1a). Thus, the removal of three aromatic residues not only enhanced the recovery from inactivation but also changed the induction of closed state inactivation towards the phenotype of KChIP1a.

Isochronal inactivation

The preceding data show that the rate of entry into and exit from the closed inactivated states was influenced by the presence of the aromatic cluster. This suggested that Kv4 channels accumulate in different closed inactivated states upon coexpression with the different KChIP1 splice variants or mutants analysed here. Wang *et al.* (2005) have shown that the various inactivated states of Kv4 are characterized by their own voltage dependence of inactivation. Therefore, we tested the isochronal inactivation properties of KChIP1a, KChIP1b and the KChIP1b-mutant 4 by selecting different inactivating intervals prior to the test pulse; the different inactivated states were separated as described by Wang *et al.* (2005). Since the first time constant of inactivation is approximately 50 ms in the presence of KChIP1a, an inactivation interval of 67 ms will largely reflect the fast inactivation process. For homomeric Kv4.2 channels the voltage dependence of inactivation with 67 ms steps resulted in a midpoint of inactivation of -21 ± 1.8 mV ($n = 7$, for detailed statistics see Table 2). Because this is a rather depolarized value and above the Kv4.2 apparent

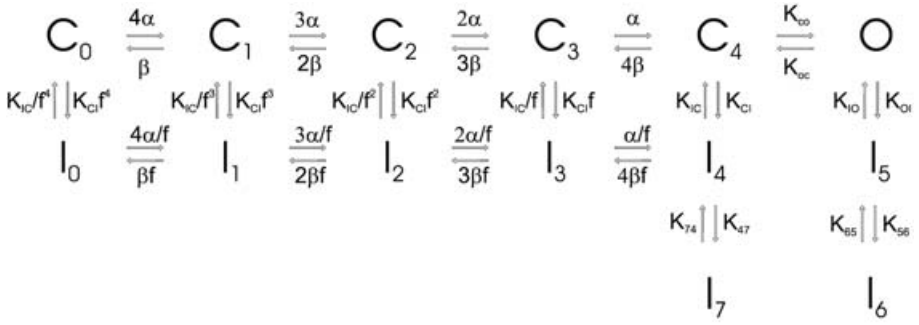

$\alpha_{(V)} = 150 \exp(0.9\, e(V/kT))$
$\beta_{(V)} = 9 \exp(-1.5\, e(V/kT))$
$k_{co,(V)} = k_{co,(V=0)} \exp(0.25\, e(V/kT))$
$k_{oc,(V)} = k_{oc,(V=0)} \exp(-0.05\, e(V/kT))$
$f = 0.3$

	Kv4.2	+ KChIP1a	+ KChIP1b
K_{CI}	7	**15**	**10**
K_{IC}	0.07	0.07	0.07
K_{OI}	80	40	40
K_{IO}	8	**16**	**10**
K_{47}	0	1	1
K_{74}	0	**20**	**0.7**
K_{56}	5	1	1
K_{65}	4	4	4
$K_{CO\,(V=0)}$	100	100	100
$K_{OC\,(V=0)}$	300	400	400

Figure 5. Gating model based on the model published by Beck *et al.* (2002)
An extra inactivated state was included and a number of rate constants were adapted to reproduce more closely our experimental data. The bottom part shows the rate constants (s^{-1}) that were used to obtain the different gating characteristics for the different expression conditions.

threshold of activation, it most likely corresponds to inactivation from the open state. In the presence of KChIP1 proteins the midpoint of inactivation determined after a 67 ms step was more negative compared to Kv4.2 alone (Fig. 7*A*, Table 2).

On the other hand, when the channels are allowed to inactivate (more) completely, they could reach a steady state distribution over the different inactivated states. When the inactivation was assessed with an inactivating step of 2000 or 5000 ms (Fig. 7*B* and *C*), we noticed that only in the presence of KChIP1b is another steady state distribution reached, compared to Kv4.2 in the presence of KChIP1a. The midpoint of inactivation in the presence of KChIP1b was significantly more hyperpolarized compared to Kv4.2 alone or in the presence of KChIP1a. Given the previous data on the inactivation kinetics, it is likely that the difference between KChIP1a and KChIP1b at 2000 and 5000 ms reflects a different distribution over distinct closed inactivated states. When three aromatic residues were mutated (Table 2), a midpoint of inactivation was obtained that was comparable to that for KChIP1a. These results show that the removal of three bulky side chains was sufficient to convert the KChIP1b phenotype (i.e. more negative midpoint of inactivation) into that of KChIP1a (i.e. a more depolarized midpoint of inactivation).

Discussion

The difference between KChIP1a and KChIP1b resides in the short but highly aromatic exon1b. We focused on the role of these aromatic residues in the distinct effects of both splice variants on the inactivation behaviour of Kv4.2 channels. The removal of three aromatic side chains resulted in restitution of the KChIP1a phenotype in terms of the distribution over the different inactivated states, the induction of prepulse inactivation and the recovery behaviour (Table 1, Figs 6 and 7). These results indicate that the presence of an aromatic cluster in KChIP1b results in a different distribution of Kv4 channels over the inactivated states that are reached from the closed state.

The effects caused by the presence of the exon1b could originate from at least two mechanisms. First, it is possible that the mere insertion of 11 extra amino acids perturbs the interactions of the remaining KChIP amino terminus, thus affecting the recovery from inactivation. However, because the removal of three aromatic side chains was sufficient to reconstitute KChIP1a recovery behaviour, we favour a second possibility: the presence of an 11 amino acid insertion, rich in bulky aromatic residues, leads to the distortion of the inactivation machinery. When a part of these bulky residues was removed, the recovery from inactivation was similar to that in the absence of the extra

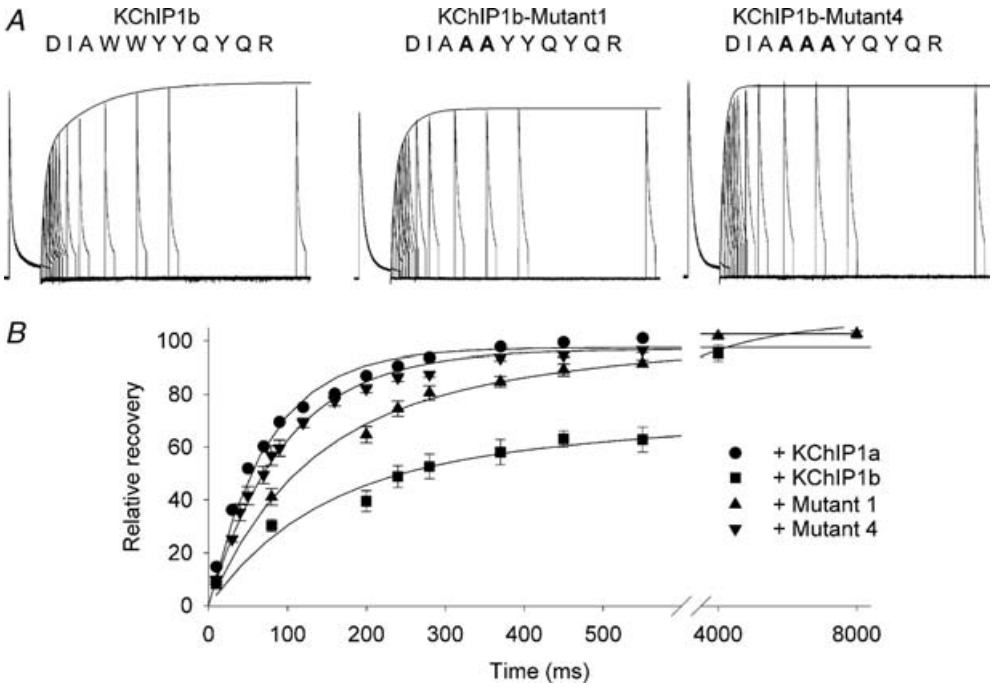

Figure 6. Recovery from inactivation for alanine mutants
A, representative current tracings for KChIP1b, Mutant 1 and Mutant 4. *B*, average normalized recovery behaviour for the different KChIP proteins transfected. Upon coexpression with KChIP1b-mutant 1 an intermediate recovery behaviour was obtained. Upon transfection of KChIP1b-Mutant 4 a single exponential recovery behaviour was seen similar to the recovery behaviour obtained with KChIP1a. The continuous lines represent exponential fits to the data.

Table 2. Voltage dependence of inactivation

	Kv4.2	KChIP1a	KChIP1b	Mutant 4
67 ms inactivation				
$V_{1/2}$ (mV)	−21.0 ± 1.8*	−30.7 ± 1.7	−29.5 ± 1.3	−28.2 ± 3.2
k	7.1 ± 0.4	7.2 ± 0.2	8.1 ± 0.8	7.8 ± 0.5
n	7	8	4	6
2000 ms inactivation				
$V_{1/2}$ (mV)	−48.5 ± 1.3*	−50.0 ± 1.3*	−55.9 ± 1.2	−48.0 ± 1.0*
k	5.5 ± 0.2	5.0 ± 0.2	6.3 ± 0.4	5.0 ± 0.3
n	9	5	3	4
5000 ms inactivation				
$V_{1/2}$ (mV)	−52.8 ± 1.0*	−50.6 ± 0.9*	−60.7 ± 3.2	−53.7 ± 1.1*
k	5.2 ± 0.3	4.3 ± 0.2	7.1 ± 0.5	4.7 ± 0.2
n	8	13	5	8

*Significant different from KChIP1b ($P < 0.05$).

exon despite the fact that 11 extra amino acids remained present.

When the KChIP1b sequence was submitted for structural prediction with different prediction programs, a variable degree of α-helical secondary structure was obtained with the border of the predicted helix varying between prediction programs. However, our results provide no independent support for such secondary structure because different combinations of substitutions that reconstituted the KChIP1a recovery behaviour displayed no obvious sidedness when the residues were projected on an α-helical wheel projection (not shown).

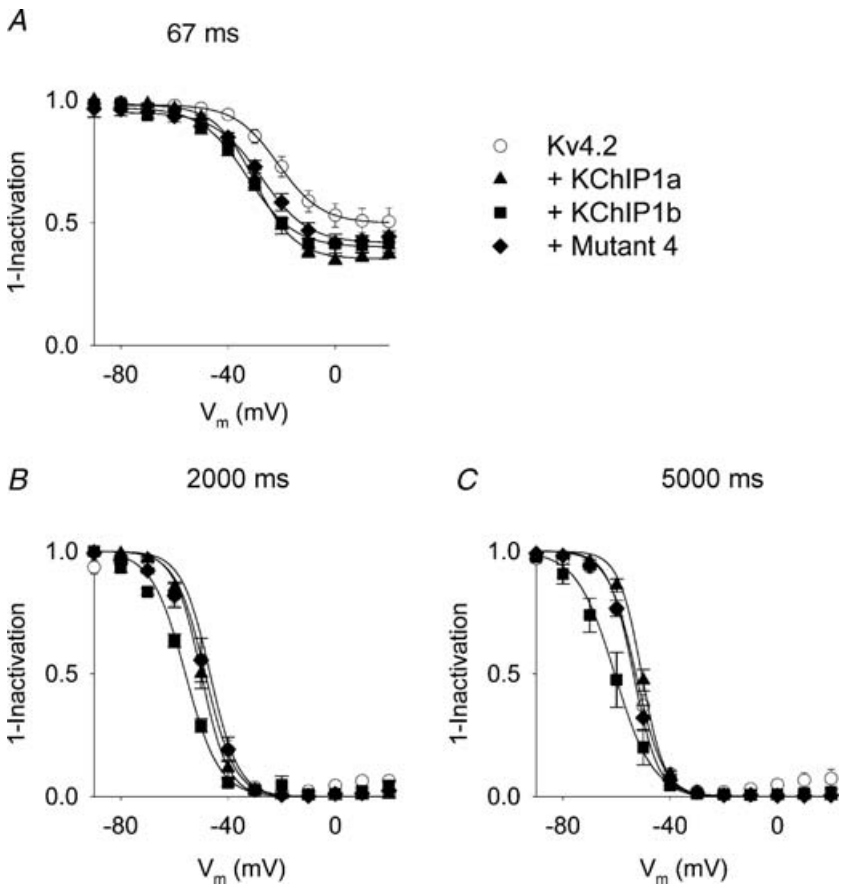

Figure 7. Isochronal inactivation of Kv4.2
A, voltage dependence of Kv4.2 inactivation after a depolarizing step of 67 ms, mainly reflecting the fast inactivation process towards the open inactivated state. The Kv4.2 midpoint of inactivation in the absence of KChIPs is more depolarized than in the presence of either KChIP subunit. *B* and *C*, upon longer depolarizing pulses of 2000 ms (*B*) and 5000 ms (*C*) the midpoint of inactivation is shifted towards hyperpolarized potentials in the presence of the KChIP1b splice variant compared to Kv4.2 alone or in the presence of KChIP1a. The continuous lines represent the Boltzmann functions calculated from the average data.

Several gating models have been proposed for Kv4 channels, all including multiple inactivated states but differing in the relative contribution and/or connectivity of the respective inactivated states. The most recent gating scheme proposed by Wang *et al.* (2005) involves five inactivated states. The most prominent feature is the inactivation from the open state and the coupling of an open-inactivated state to a closed inactivated state. While this model reproduces many Kv4.2 gating features it fails to simulate the voltage dependence of recovery with a very slow recovery from inactivation at −90 mV, as recognized by the authors. Since we focused on differences in the recovery behaviour, this model was not applicable to our results. In previous models inactivation from pre-open closed states was combined with a reverse-biased opening step. In these models the Kv4 channels accumulate in a closed inactivated state upon a long depolarizing step and recover fast from this state with a single exponential process (Bahring *et al.* 2001*b*; Beck *et al.* 2002). Moreover, recent evidence suggests that the inactivated state of Kv4 is structurally related to the closed state (Wang & Covarrubias, 2006).

The recent structural data on the binding of KChIPs to the Kv4 channels indicate that the Kv4 N-terminus is at least less available for inducing open state inactivation as it is bound by the KChIPs (Pioletti *et al.* 2006; Wang *et al.* 2007). Under the assumption that the N-terminus is largely involved in the open state inactivation process (Bahring *et al.* 2001*a*; Gebauer *et al.* 2004), its binding by KChIPs correlates with the reduction of the contribution of the fast time constant in the inactivation kinetics. However, contrary to some reports, we and others still observed multiple exponential inactivation kinetics in the presence of KChIP1.*x* (Nakamura *et al.* 2001; Boland *et al.* 2003). Therefore, the virtual elimination of the open state inactivation pathway by a very large decrease of the k_{OI} rate constant is not appropriate (Beck *et al.* 2002). Based upon these observations the open state inactivation process is either not solely due to the Kv4 N-terminus or the KChIPs bound to the Kv4 channel intermittently release the Kv4 N-terminus making it free for inducing fast open state inactivation. It has also been shown that the removal of a part of the Kv4 N-terminus slows inactivation although it remains a multiple exponential process (Bahring *et al.* 2001*a*). For these reasons we lowered the k_{OI} rate in our model but to a lesser extent than published.

The inclusion of the I_7 state was based on our observation that KChIP1a and KChIP1b differ in their voltage dependence of inactivation upon application of longer depolarizing pulses (5 s). Moreover, the midpoints for both splice variants were far below the apparent threshold of activation indicating that it is unlikely that the open state inactivation pathway would be involved. Furthermore, inactivation from the closed state is usually described by a mono-exponential time course. However, we observed that the coexpression of KChIP1b resulted in a double exponential time course of closed state inactivation suggesting a distribution over at least two closed inactivated states with distinct recovery kinetics. This biexponential recovery occurred after both 1 s and 5 s depolarizing pulses (Supplemental Fig. 1), which further supports the inclusion of the I_7 state.

In conclusion, we were able to demonstrate that the presence of a large bulky cluster in the amino terminus of KCHIP1b slowed the recovery from inactivation and changed the distribution over closed inactivated states. The reduction of the aromatic cluster by replacement of three aromatic residues sufficed to obtain fast recovery from inactivation, as seen in the absence of exon1b (KChIP1a).

References

An WF, Bowlby MR, Betty M, Cao J, Ling HP, Mendoza G, Hinson JW, Mattsson KI, Strassle BW, Trimmer JS & Rhodes KJ (2000). Modulation of A-type potassium channels by a family of calcium sensors. *Nature* **403**, 553–556.

Bahring R, Boland LM, Varghese A, Gebauer M & Pongs O (2001*a*). Kinetic analysis of open- and closed-state inactivation transitions in human Kv4.2 A-type potassium channels. *J Physiol* **535**, 65–81.

Bahring R, Dannenberg J, Peters HC, Leicher T, Pongs O & Isbrandt D (2001*b*). Conserved Kv4 N-terminal domain critical for effects of Kv channel-interacting protein 2.2 on channel expression and gating. *J Biol Chem* **276**, 23888–23894.

Beck EJ, Bowlby M, An WF, Rhodes KJ & Covarrubias M (2002). Remodelling inactivation gating of Kv4 channels by KChIP1, a small-molecular-weight calcium-binding protein. *J Physiol* **538**, 691–706.

Beck EJ & Covarrubias M (2001). Kv4 channels exhibit modulation of closed-state inactivation in inside-out patches. *Biophys J* **81**, 867–883.

Boland LM, Jiang M, Lee SY, Fahrenkrug SC, Harnett MT & O'Grady SM (2003). Functional properties of a brain-specific NH_2-terminally spliced modulator of Kv4 channels. *Am J Physiol Cell Physiol* **285**, C161–C170.

Decher N, Barth AS, Gonzalez T, Steinmeyer K & Sanguinetti MC (2004). Novel KChIP2 isoforms increase functional diversity of transient outward potassium currents. *J Physiol* **557**, 761–772.

Decher N, Uyguner O, Scherer CR, Karaman B, Yuksel-Apak M, Busch AE, Steinmeyer K & Wollnik B (2001). hKChIP2 is a functional modifier of hKv4.3 potassium channels: cloning and expression of a short hKChIP2 splice variant. *Cardiovasc Res* **52**, 255–264.

Gebauer M, Isbrandt D, Sauter K, Callsen B, Nolting A, Pongs O & Bahring R (2004). N-type inactivation features of Kv4.2 channel gating. *Biophys J* **86**, 210–223.

Hamill OP, Marty A, Neher E, Sakmann B & Sigworth FJ (1981). Improved patch clamp techniques for high-resolution current recording from cells and cell-free membrane patches. *Pflugers Arch* **391**, 85–100.

Hoffman DA, Magee JC, Colbert CM & Johnston D (1997). K^+ channel regulation of signal propagation in dendrites of hippocampal pyramidal neurons. *Nature* **387**, 869–875.

Holmqvist MH, Cao J, Hernandez-Pineda R, Jacobson MD, Carroll KI, Sung MA, Betty M, Ge P, Gilbride KJ, Brown ME, Jurman ME, Lawson D, Silos-Santiago I, Xie Y, Covarrubias M, Rhodes KJ, Distefano PS & An WF (2002). Elimination of fast inactivation in Kv4 A-type potassium channels by an auxiliary subunit domain. *Proc Natl Acad Sci U S A* **99**, 1035–1040.

Jerng HH, Kunjilwar K & Pfaffinger PJ (2005). Multiprotein assembly of Kv4.2, KChIP3 and DPP10 produces ternary channel complexes with ISA-like properties. *J Physiol* **568**, 767–788.

Jerng HH, Pfaffinger PJ & Covarrubias M (2004). Molecular physiology and modulation of somatodendritic A-type potassium channels. *Mol Cell Neurosci* **27**, 343–369.

Nadal MS, Ozaita A, Amarillo Y, De Miera EV, Ma Y, Mo W, Goldberg EM, Misumi Y, Ikehara Y, Neubert TA & Rudy B (2003). The CD26-related dipeptidyl aminopeptidase-like protein DPPX is a critical component of neuronal A-type K^+ channels. *Neuron* **37**, 449–461.

Nakamura TY, Nandi S, Pountney DJ, Artman M, Rudy B & Coetzee WA (2001). Different effects of the Ca^{2+}-binding protein, KChIP1, on two Kv4 subfamily members, Kv4.1 and Kv4.2. *FEBS Lett* **499**, 205–209.

Patel SP, Campbell DL & Strauss HC (2002). Elucidating KChIP effects on Kv4.3 inactivation and recovery kinetics with a minimal KChIP2 isoform. *J Physiol* **545**, 5–11.

Patel SP, Parai R, Parai R & Campbell DL (2004). Regulation of Kv4.3 voltage-dependent gating kinetics by KChIP2 isoforms. *J Physiol* **557**, 19–41.

Pioletti M, Findeisen F, Hura GL & Minor DL Jr (2006). Three-dimensional structure of the KChIP1-Kv4.3, T1 complex reveals a cross-shaped octamer. *Nat Struct Mol Biol* **13**, 987–995.

Radicke S, Cotella D, Graf EM, Ravens U & Wettwer E (2005). Expression and function of dipeptidyl-aminopeptidase-like protein 6 as a putative β-subunit of human cardiac transient outward current encoded by Kv4.3. *J Physiol* **565**, 751–756.

Schoppa NE & Westbrook GL (1999). Regulation of synaptic timing in the olfactory bulb by an A-type potassium current. *Nat Neurosci* **2**, 1106–1113.

Van Hoorick D, Raes A, Keysers W, Mayeur E & Snyders DJ (2003). Differential modulation of Kv4 kinetics by KCHIP1 splice variants. *Mol Cell Neurosci* **24**, 357–366.

Wang S, Bondarenko VE, Qu YJ, Bett GC, Morales MJ, Rasmusson RL & Strauss HC (2005). Time- and voltage-dependent components of Kv4.3 inactivation. *Biophys J* **89**, 3026–3041.

Wang G & Covarrubias M (2006). Voltage-dependent Gating Rearrangements in the intracellular T1–T1 interface of a K^+ channel. *J Gen Physiol* **127**, 391–400.

Wang H, Yan Y, Liu Q, Huang Y, Shen Y, Chen L, Chen Y, Yang Q, Hao Q, Wang K & Chai J (2007). Structural basis for modulation of Kv4 K^+ channels by auxiliary KChIP subunits. *Nat Neurosci* **10**, 32–39.

Yeola SW & Snyders DJ (1997). Electrophysiological and pharmacological correspondence between Kv4.2 current and rat cardiac transient outward current. *Cardiovasc Res* **33**, 540–547.

Yuste R (1997). Potassium channels – dendritic shock absorbers. *Nature* **387**, 851.

Acknowledgements

This work was supported by the 'Fonds voor Wetenschappelijk Onderzoek Vlaanderen' Grant FWO-G.0152.06 and G.0035.05, the IAP6/31 of the Interuniversity Attraction Poles Program – Belgian State – Belgian Science Policy and a concerted research project Grant GOA 2004 of the University of Antwerp.

Supplemental material

Online supplemental material for this paper can be accessed at:
http://jp.physoc.org/cgi/content/full/jphysiol.2007.139550/DC1
and
http://www.blackwell-synergy.com/doi/suppl/10.1113/jphysiol.2007.139550